Talanta 201 (2019) 90–95

Contents lists available at ScienceDirect

Talanta

journal homepage: www.elsevier.com/locate/talanta

Construction of FRET biosensor for off-on detection of lead ions based on carbon dots and gold nanorods

Guoliang Liu[a,b,*], Da-Qian Feng[b], Yanling Qian[c], Wei Wang[b], Jun-Jie Zhu[a,**]

[a] State Key Laboratory of Analytical Chemistry for Life Science, School of Chemistry and Chemical Engineering, Nanjing University, Nanjing, Jiangsu, 210093, China
[b] School of Chemistry and Chemical Engineering, Yancheng Institute of Technology, Jiangsu, 224051, China
[c] School of Information Science and Engineering, Lanzhou University, Gansu, 730000, China

ARTICLE INFO

Keywords:
Off-on biosensor
Carbon dots
Gold nanorods
Fluorescence resonance energy transfer
Lead ions detection

ABSTRACT

Exploring new energy donor/acceptor pairs for constructing FRET system has important research significance. In this study, a FRET assembly by using carbon dots (CDs) as energy donor and gold nanorods (Au NRs) as energy acceptor has been proposed through covalent bond interactions by taking advantage of cysteamine as a bridge. The assembly is characterized by UV–vis absorption spectra, fluorescence spectra, FT-IR spectra and TEM images, revealing that Au NRs successfully absorbed on the surface of CDs. As for the occurrence of FRET process from CDs to Au NRs, the fluorescence signal of CDs-cysteamine-Au NRs assembly quenched significantly. Interestingly, Pb^{2+} ions could bind completely with cysteamine and disturbed the FRET process, which activated fluorescence signal of the system. Based on these experimental phenomena, CDs-cysteamine-Au NRs assembly was performed as an off-on FRET biosensor for Pb^{2+} ions. The linear range obtained is from 0 to 155 μM with the detection limit of 0.05 μM. Moreover, the FRET-based sensor exhibited high selectivity to the analyte Pb^{2+} ions against other interference substances. Furthermore, the present approach was successfully applied to detect Pb^{2+} ions in real samples, which suggested its potential applications in environmental monitoring.

1. Introduction

Forster resonance energy transfer (FRET) is a powerful tool for recognizing subtle changes related to molecular recognition behavior [1–3]. FRET is a non-radiative energy transfer from an excited donor to a ground-state acceptor in close proximity via Coulomb interactions, which leads to a fluorescence quenching phenomenon [4,5]. The distance between energy pairs is typically less than 10 nm [6]. Energy donor/acceptor pairs play a crucial role for the performance of FRET assays except for the distance [7]. However, it lacks the effective energy donor/acceptor pairs currently. Therefore, it is a great important to explore the new energy donor/acceptor pairs for constructing FRET system.

Carbon dots (CDs), one kind of new fluorescent nanomaterials, are attracting increasing attention in the past decade due to their unique optical properties, environmental friendliness, good biocompatibility, tunable emission spectrum, and facile synthesis [8–10]. As the surface of CDs possess large amount of carboxyl and hydroxyl groups, prepared CDs have the favorable potential for post-modified chemical groups. Since their discovery, CDs have been applications in the fields of chemical sensing, biosensing, nanomedicine, bioimaging, and so on [11–15]. At present, there are only few works reported by using CDs as the donor [16]. Therefore, the study on CDs-based FRET probes possesses important significance.

Gold nanorods (Au NRs) have wide range applications in biology and biomedicine fields due to the exceptional surface plasmon resonance property [17–19]. Besides, Au NRs are usually performed as the nanocarrier for loading various objects to construct multifunctional nanoprobes due to high specific surface area [20,21]. In light of the strong fluorescence quenching ability, we can expect it to be as energy acceptor to improve the performance of FRET-based probe to a large extent.

Herein, a new label-free FRET-based assay for sensing environmental pollutant heavy metal Pb^{2+} ions was proposed by using CDs as energy donor and Au NRs as energy acceptor. Scheme 1 displayed that the cysteamine was selected as a bridge between CDs and Au NRs for constructing effective FRET system. As cysteamine had amino group and sulfhydryl group, the formation of amido bond between amino

* Corresponding author. School of Chemistry and Chemical Engineering, Yancheng Institute of Technology, Jiangsu 224051, China.
** Corresponding author. State Key Laboratory of Analytical Chemistry for Life Science, School of Chemistry and Chemical Engineering, Nanjing University, Nanjing, Jiangsu, 210093, China.
E-mail addresses: glliu@ycit.edu.cn, liuguoliang199@126.com (G. Liu), jjzhu@nju.edu.cn (J.-J. Zhu).

https://doi.org/10.1016/j.talanta.2019.03.101
Received 10 December 2018; Received in revised form 19 March 2019; Accepted 30 March 2019
Available online 01 April 2019
0039-9140/

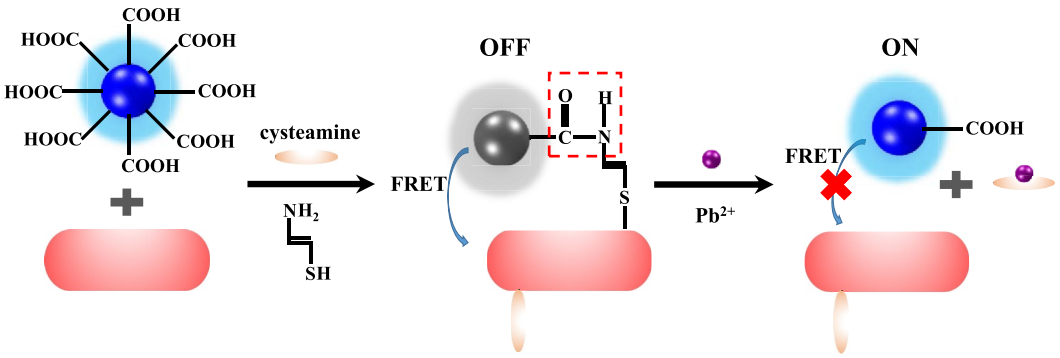

Scheme 1. Schematic illustration of the construction of FRET assembly by using carbon dots and gold nanorods and their application as an off-on fluorescent detection of Pb^{2+} ions.

group of cysteamine and carboxyl group on the surface of CDs and the formation of Au—S bond between sulfhydryl group of cysteamine and Au NRs produced the CDs-cysteamine-Au NRs assembly together. Moreover, CDs-cysteamine-Au NRs assembly based biosensor was applied for quantitatively detecting heavy metal Pb^{2+} ions (Scheme 1). CDs-cysteamine-Au NRs assembly exhibited weak fluorescence signal due to FRET mechanism, called as OFF. Upon the introduction of Pb^{2+} ions, the complexation between cysteamine and lead ions would lead to the disturbance behavior of FRET process, which induced activatable fluorescence signal of the biosensor, named as ON. A biosensor typically consists of a molecular recognition part (sensitive element) and a conversion part (transducer). In our assay, cysteamine is selected as a molecular recognition part of our developed sensor while the CDs-cysteamine-Au NRs assembly is used as a conversion part. Upon the addition of the analyte Pb^{2+} ions, the CDs-cysteamine-Au NRs assembly is able to transduce the molecular recognition behavior between the cysteamine and Pb^{2+} ions into an optical signal. As the concentration of Pb^{2+} ions increased, the fluorescence intensity of the system gradually enhanced. Thus, a facile and label-free FRET-based approach of detecting Pb^{2+} ions was developed. The analytical performance of the biosensor was investigated systematically. Furthermore, the present FRET-based approach was successfully applied to detect Pb^{2+} ions in local river samples with satisfied results.

2. Experimental

2.1. Materials

Ascorbic acid, citric acid, sodium borohydride and hexadecyltrimethylammonium bromide (CTAB, 99%) were obtained from Aladdin industrial corporation (China). Silver nitrate was obtained from Shanghai Fine Chemical Materials Research Institute (China). Sodium hydroxide and hydrochloric acid were purchased from Shanghai Lingfeng Chemical Reagent Co. Ltd. (China). Sodium oleate, tetrachloroauric (III) acid hydrate, cysteamine, lead nitrate, and other reagents were all purchased from Sinopharm Chemical Reagent Co. Ltd (China). All reagents were of analytical grade and used without further purification. The ultrapure water with 18.2 MΩ cm^{-1} was used throughout the whole experiments.

2.2. Instruments and characterizations

UV–vis absorption spectra were carried out on a Shimadzu 245 UV–vis spectrophotometer (Shimadzu, Japan). The fluorescence spectra were recorded with a model Jasco FP-6500 fluorescence spectrometer (Jasco, Japan). Transmission electron microscopy (TEM) images were recorded on a field emission transmission electron microscope at an accelerating voltage of 200 kV (JEM-2100F, JEOL, Ltd., Japan). Fourier transform-infrared (FT-IR) spectra were obtained by using a Nicolet-6700 FT-IR spectrometer (Thermo Ltd., USA) within a range of 400–4000 cm^{-1}.

2.3. Procedures

2.3.1. Synthesis of water-soluble carbon dots

Water-soluble carbon dots (CDs) were synthesized by one-pot method in the light of the literature with little modification [22]. First, the temperature of the oven was adjusted to 200 °C. After that, the 25 mL beaker was added into 2 g citric acid anhydrous powder and quickly put into the oven. Accompanied by the time, the solid powder gradually becomes liquid. Meanwhile, the color of the product changes from colorless to orange. After sustained heating for 1 h, the beaker was taken out and cooled to ambient temperature naturally. After vigorous stirring for 5 min, NaOH (10 mg/mL) solution was added drop by drop to adjust the pH value of the product to 7. The supernatants were further purified through a dialysis membrane tubing (3500 Da, molecular weight cut-off, Viskase). The final solution was stored in a refrigerator at 4 °C for further research.

2.3.2. Preparation of gold nanorods

Gold nanorods (Au NRs) were prepared according to the improved seed-mediated growth method of our reported work [23]. Firstly, the seed growth solution was synthesized as follows: The $HAuCl_4$ solution (2 mL, 0.5 mM) was added into 2 mL CTAB solution (0.2 M) in a 10 mL test tube. After that, 0.4 mL $NaBH_4$ (0.06 M, freshly prepared and ice-cold) solution was introduced in the tube under vigorous stirring for 2 min. The seed growth solution was kept at 25 °C before using. Secondly, CTAB (0.56 g) and sodium oleate (0.10 g) were added into a 50 mL round-bottomed flask and then 20 mL ultrapure water was added. The flask was kept in a water bath under 50 °C for about 30 min, then cool down to 30 °C. After that, 1.92 mL $AgNO_3$ solution (4 mM) was introduced into flask and was kept at 30 °C for 15 min. Then, 20 mL $HAuCl_4$ solution (1 mM) was added into the mixture and was kept stirring in intermediate speed for another 90 min. The color of the mixture solution changed from dark yellow to colorless. Next, 0.17 mL HCl solution (37 wt % in water, 12.1 M) was then added to adjust the pH value of the mixture and then slow stirring for 15 min. After that, 0.10 mL ascorbic acid (0.06 M, freshly prepared) was added and the mixture solution was vigorously stirred for 30 s. Then, 64 μL the seed growth solution was added with stirred for another 30 s. The obtained produce solution was left undisturbed at 30 °C over night. The concentration of prepared Au NRs was determined by using inductively coupled plasma atomic emission spectrometer (ICP-AES) (0.65 nM) [24].

2.3.3. Detection of Pb^{2+} ions

The Au NRs solution was diluted to 5 mL with Britton-Robinson buffer solution (BR buffer) and then mixed with certain concentration

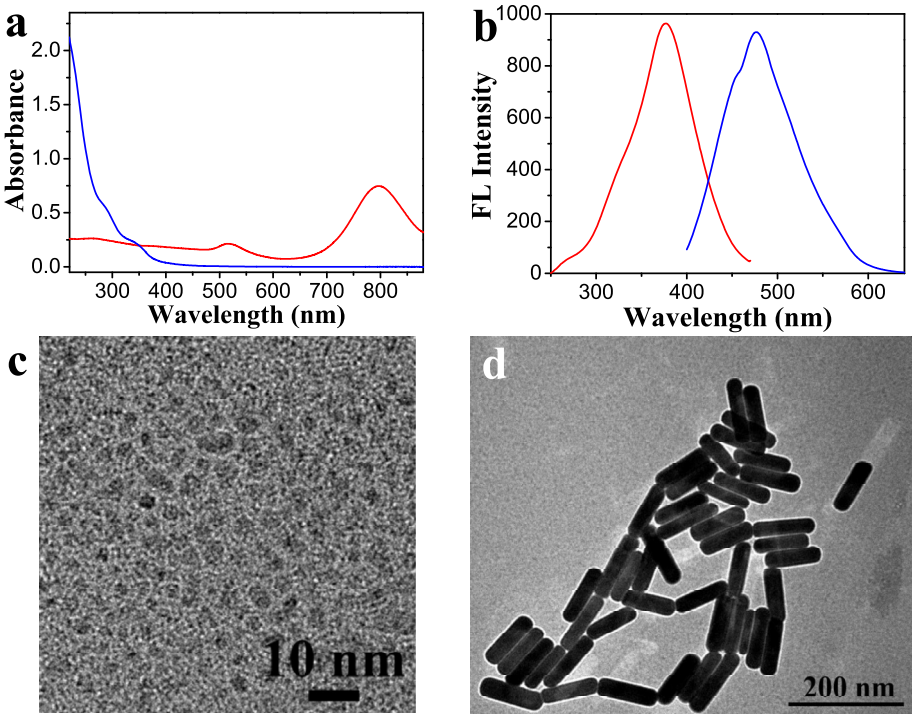

Fig. 1. (a) UV–vis absorption spectra of pre-prepared CDs (blue line) and Au NRs (red line); (b) The fluorescent excitation (red line) and emission (blue line) spectra of synthesized CDs; (c) Typical High-Resolution Transmission Electron Microscope (HR-TEM) image of CDs; (d) Typical Transmission Electron Microscope (TEM) image of prepared Au NRs. (For interpretation of the references to color in this figure legend, the reader is referred to the Web version of this article.)

of cysteamine solution. The reaction was kept for certain minutes at room temperature. Then, certain concentration of CDs solution was introduced. After that, the mixture solution was added into different concentrations of analyte Pb^{2+} ions solution. After 1 min, the fluorescent spectra of the reactive solution were measured by fluorescence spectrometer with slit width at 5 nm at room temperature [25]. The excitation wavelength was set up at 377 nm.

3. Results and discussion

3.1. Characterization of the CDs and Au NRs

The carbon dots (CDs) were synthesized according to the reported method with a little modification [22]. The UV–vis spectrum of pre-pared CDs showed a typical broad absorption at 345 nm (the blue line in Fig. 1a). Meanwhile, the gold nanorods (Au NRs) were prepared by using improved seeding-mediated growth method [23]. The surface plasmon resonance spectrum of synthesized Au NRs is displayed in the red line in Fig. 1a. The longitudinal plasmon wavelength of as-prepared Au NRs is around 800 nm and the transverse plasmon wavelength is 516 nm, demonstrating the successful synthesis of Au NRs [20]. The prepared CDs exhibited the maximum emission peak located at 478 nm when the excitation wavelength was set up at 377 nm (Fig. 1b), suggesting the synthesis of CDs [13]. Besides, typical High-Resolution Transmission Electron Microscope (HR-TEM) image revealed that the prepared CDs were mono-dispersive with the uniform size of 3 nm by the inserted image (Fig. 1c). The pre-prepared Au NRs were also characterized by using transmission electron microscopy (TEM) where both the size and morphology of synthesized Au NRs were exhibited clearly. The images revealed that the Au NRs possessed uniform morphology with 100 ± 4 nm long axis size and 28 ± 3 nm short axis size, further revealing successful preparation of Au NRs (Fig. 1d).

3.2. Optimization of experimental conditions

The experimental conditions including the concentration of gold nanorods, pH value, and response time were investigated. As shown in Fig. S1, the effect of pH value of the reactive solution on the system including CDs, CDs/Au NRs, CDs-cysteamine-Au NRs is not obvious because fluorescent intensity of the system did not appear significant change in the whole tested pH value ranges from 4.0 to 10.0. However, the effect pH value on the detection Pb^{2+} ions system based on CDs-cysteamine-Au NRs was visible. Especially, the increment of fluorescence intensity reached maximum value (compared blue line with violet line) when pH value was at 7.4. Thus, pH 7.4 was chosen for further experimental assays. Under the optimum conditions, the effect of incubation time on fluorescence intensity of CDs-cysteamine-Au NRs system in the presence of Pb^{2+} ions was tested. The assay incubation time was also studied by determining fluorescent intensity of the system every 1 min for 10 min immediately after mixing (Fig. S2). The results showed that the reaction between CDs-cysteamine-Au NRs system and Pb^{2+} ions occurred rapidly at room temperature and the fluorescence intensity of the reactive system reached the maximum. Hence, this assay did not require crucial timing. The optimum incubation time was 1 min. As displayed in Fig. S3, the concentration of Au NRs possessed a significant influence on the fluorescence intensity of the assay system. With the addition of Au NRs, the fluorescence intensity of the synthesized CDs decreased and kept the constant when the concentration was more than 24 pM. To further order to clearly observe the changing trend, the curve was made and listed in Fig. S4. Therefore, 24 pM Au NRs was selected in this study.

3.3. The fluorescence turn-on detection of Pb^{2+} ions by using CDs-cysteamine-Au NRs assembly

To construct energy transfer system, fluorescent CDs and Au NRs were selected as electron donor and acceptor. Cysteamine was used as a bridge for developing fluorescence resonance energy transfer as for having amino group and sulfhydryl group. First, the formation of amido bond between amino group and carboxyl group on the surface of CDs produced cysteamine functionalized CDs complex (CDs-cysteamine). After that, Au NRs adsorbed on the surface of CDs-cysteamine complex due to the formation of S—Au bond, which formed CDs-cysteamine-Au NRs assembly. The fluorescence signal of CDs-cysteamine-Au NRs assembly significantly quenched due to the occurrence of fluorescence resonance energy transfer process, named as “OFF” state. Interestingly,

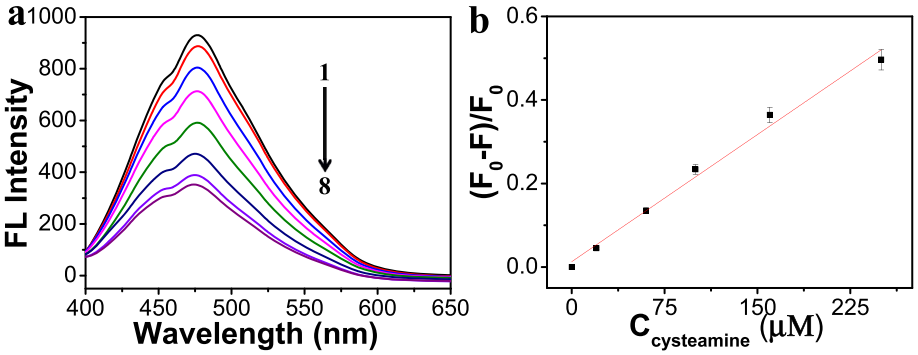

Fig. 2. (a) Fluorescence emission spectra of CDs/Au NRs assembly in the absence and presence of different amounts of cysteamine. Conditions: 1, CDs/Au NRs assembly; 2–8: 1 + cysteamine (μM): 20, 60, 100, 160, 250, 350, 500. (b) The linear correlation between $(F_0\text{-}F)/F_0$ and the concentrations of cysteamine.

upon the addition of the analyte Pb^{2+} ions, the energy transfer process was disturbed due to the competitive combination between cysteamine and Pb^{2+} ions. Then, the fluorescence signal of CDs-cysteamine-Au NRs assembly recovered, called as "ON" state. Thus, the assembly was applied as a new turn-on fluorescent probe for sensitively detecting Pb^{2+}.

The fluorescence spectra of CDs/Au NRs assembly in the absence and presence of cysteamine are shown in Fig. 2a. The assay results reveal that strong fluorescence signal of CDs/Au NRs assembly decreased remarkably upon the addition of cysteamine. It was ascribed to the fact that cysteamine was a bridge for constructing fluorescence resonance energy transfer system due to its having amino group and sulfhydryl group. The energy transfer process led to the remarkably quenching fluorescence of CDs/Au NRs assembly. As the increasing concentration of cysteamine, the fluorescence intensity of CDs was gradually quenched. The relationship between $(F_0\text{-}F)/F_0$ (F_0 and F is the fluorescence intensity of CDs/Au NRs in the absence and presence of cysteamine, respectively) and the concentration of cysteamine is displayed in Fig. 2b. The linear range is from 0 to 250 μM with the detection limit 0.2 μM. The linear equation was expressed as $(F_0\text{-}F)/F_0 = 0.002 + 0.012C_{cysteamine}$ (r = 0.9950).

The CDs-cysteamine-Au NRs assembly is further applied to efficiently determining Pb^{2+} ions. As displayed in Fig. S5, the CDs/Au NRs assembly exhibits quite strong fluorescence signal (curve 1), the introduction of Pb^{2+} ions nearly doesn't change the fluorescence signal (data is not listed). However, the quenched fluorescence signal of CDs-cysteamine-Au NRs assembly (curve 2) is effectively activated after the addition of Pb^{2+} ions solution (curve 3). The detailed data are listed in Table S1. The fluorescent recovery rate is also calculated (75.7%). Thus, experimental assays suggest that the addition of the analyte Pb^{2+} ions don't change the fluorescence intensity of the CDs/Au NRs assembly in the absence of cysteamine, which provide the possibility of the present sensor's application in detecting Pb^{2+} ions.

Fig. 3a displays the fluorescence emission spectra of CDs-cysteamine-Au NRs assembly in the presence of different amounts of Pb^{2+} ions. It is observed that the fluorescent emission intensity of CDs-cysteamine-Au NRs assembly is effectively activated in the presence of the analyte. Moreover, the fluorescence intensity increased gradually with the increasing concentration of Pb^{2+} ions (Fig. 3a). The plot of the relative fluorescence intensity $(F\text{-}F_0)/F_0$ versus the concentrations of Pb^{2+} ions is observed in the range from 0 μM to 155 μM (Fig. 3b). The linear equation is expressed as $(F\text{-}F_0)/F_0 = 0.024 + 0.008C_{Pb}{}^{2+}$ (r = 0.9984). The limit of detection ($3\sigma/K$) for sensing Pb^{2+} ions is 0.05 μM (σ is the standard deviation of nine measurements, and K is the slope of the range of the linearity). Therefore, the CDs-cysteamine-Au NRs assembly is suitable for turn-on detecting trace amounts of Pb^{2+} ions.

3.4. Fluorescence response mechanism of CDs-cysteamine-Au NRs assembly to Pb^{2+} ions

It is well-known that the energy transfer system can be formed when fluorescence excitation spectrum of the electron donor and the UV–vis spectrum of the electron acceptor are overlapped. Fig. 4 displays that there is an overlap between fluorescence excitation peak of CDs and UV–vis absorption peak of short axis of Au NRs, which demonstrates the possibility of constructing FRET system by using C-dots and gold nanorods as donor and acceptor, respectively.

In order to further explore the mechanism of the proposed FRET system, Fourier transform-infrared (FT-IR) spectrum was carried out. Fig. 5a displays FT-IR spectra of prepared CDs, Au NRs and the mixture solution of CDs-Au NRs. The peak of C—H stretching vibration is located at 2950 cm^{-1} while that of O—H stretching vibration is at 3450 cm^{-1}. The peak of COO^- stretching vibration is at 1630 cm^{-1} and 1450 cm^{-1}. Compared with curve 1, the addition of gold nanorods has little effect on the surface group of CDs in curve 3 of Fig. 5a. The infrared comparison figures of CDs/Au NRs system in the presence of cysteamine and analyte Pb^{2+} ions are clearly displayed in Fig. 5b. The curve 2 shows the FT-IR spectrum of cysteamine, revealing the peak of S—H stretching vibration is located at 2550 cm^{-1}. It is observed that the addition of cysteamine induces the appearance of S—H stretching

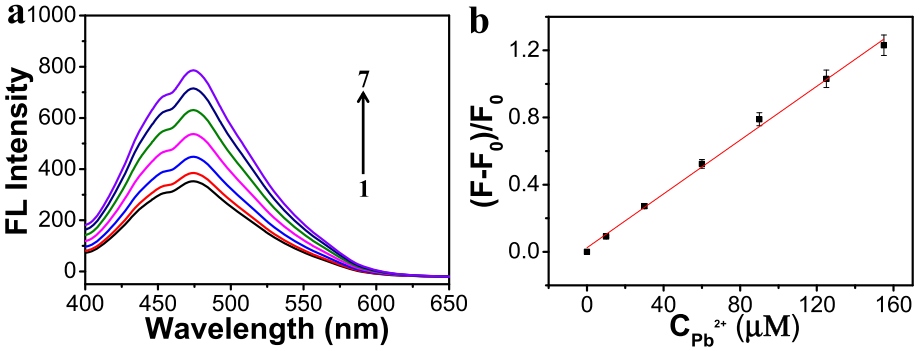

Fig. 3. (a) Fluorescence emission spectra of CDs-cysteamine-Au NRs assembly in the absence and presence of different amounts of Pb^{2+} ions. Conditions: 1, CDs-cysteamine-Au NRs assembly; 2–7: 1 + Pb^{2+} ions (μM): 10, 30, 60, 90, 125, 155. The concentration of cysteamine is 500 μM. (b) The linear correlation between $(F\text{-}F_0)/F_0$ and the concentrations of analyte Pb^{2+} ions.

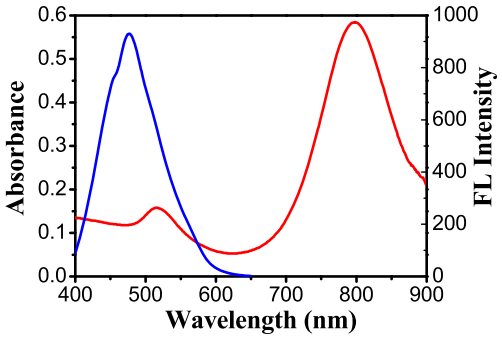

Fig. 4. Absorption spectrum of synthesized Au NRs (red line) and fluorescence emission spectrum of prepared CDs (blue line). (For interpretation of the references to color in this figure legend, the reader is referred to the Web version of this article.)

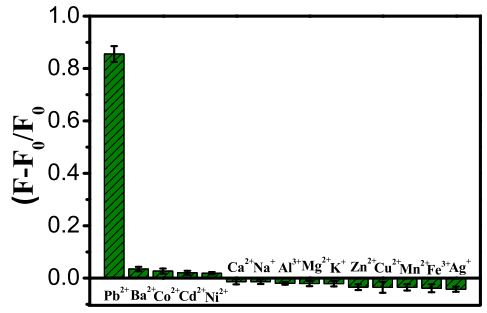

Fig. 6. Fluorescence response of CDs-cysteamine-AuNRs assembly to Pb^{2+} ions or other various metal cations. The concentration of Pb^{2+} is 130 μM. The concentrations of K^+ and Na^+ are 1 mM. The concentrations of Ba^{2+}, Co^{2+} and Cd^{2+} are 0.1 mM. Other cations concentrations are 0.5 mM. The concentration of cysteamine is 500 μM.

vibration peak in curve 3 in comparison with those of curve 1 and 2, suggesting the formation of Au—S bond on the surface of Au NRs. So it is speculated that the fluorescence quenching mechanism of CDs is due to the addition of cysteamine, which plays an important role of a bridge between energy donor CDs and energy accept Au NRs and forms CDs-cysteamine-Au NRs assembly. As the CDs is close to Au NRs, the FRET behavior from CDs to Au NRs occurs, which results in quenching fluorescence signal of CDs-cysteamine-Au NRs assembly. From the comparison of curve 3 and curve 4 of Fig. 5b, the introduction of Pb^{2+} ions disturbs S—Au bond due to competitive binding effect between Pb^{2+} ions and cysteamine, inducing Au NRs separating from CDs and turning-on fluorescence signal of reactive system. Moreover, to further explore the nature of binding behavior, measurements of surface charge assays were also implemented (Table S2). The experimental results revealed that the introduction of Pb^{2+} ions induced Zeta potential of CDs-cysteamine-Au NRs assembly becoming more negative, which verified the disassembly behavior. Thus, electrostatic interaction also contributes to the assembly and disassembly behavior of CDs-cysteamine-Au NRs.

3.5. The selectivity assay of Pb^{2+} ions detection by CDs-cysteamine-Au NRs assembly

In order to investigate the selectivity of the established CDs-cysteamine-Au NRs assembly based sensing system, the fluorescent response of the approach to other metal ions was also investigated under the same conditions as in the case of Pb^{2+} ions. The metal ions including Ba^{2+}, Co^{2+}, Cd^{2+}, Ni^{2+}, Ca^{2+}, Na^+, Al^{3+}, Mg^{2+}, K^+, Zn^{2+}, Cu^{2+}, Mn^{2+}, Fe^{3+}, Ag^+ were tested. As shown in Fig. 6, the fluorescence quenching efficiency of Pb^{2+} ions to CDs-cysteamine-Au NRs assembly sensing system is significant, whereas no obvious fluorescent signal change is observed for other metal ions under the identical conditions. The experimental results demonstrate that the proposed system has high selectivity for Pb^{2+} ions detection against other metal ions. Therefore, the CDs-cysteamine-Au NRs assembly sensing system has the potential application for detecting Pb^{2+} ions in real samples.

3.6. Analysis of Pb^{2+} ions in real samples

To further demonstrate the feasibility of the proposed FRET system for real sample determination, the CDs-cysteamine-Au NRs assembly based fluorescent sensor is performed to detect Pb^{2+} ions in tap water and river water samples. A standard addition method was adopted to detect the concentration of Pb^{2+} ions in environmental water samples from local Tongyu river water. The results obtained by the proposed CDs-cysteamine-Au NRs assembly sensor are compared with those obtained by the traditional HPLC method (Table 1). The analytical results suggest that good consistency is observed between two methods, indicating that the proposed CDs-cysteamine-Au NRs assembly sensor can be applied to analyze Pb^{2+} ions in environmental monitoring. Table S3 compares our present approach with other reported methods including colorimetric, electrochemical and fluorescence sensors for the detection of Pb^{2+} ions with respect to detection limit and linear range [26–29]. Our proposed sensor exhibits wider linear range and comparable detection limit.

4. Conclusion

In summary, the FRET-based sensing system was developed for fluorescent detection of heavy metal Pb^{2+} ions based on CDs-cysteamine-Au NRs assembly. The pre-prepared CDs were used as the energy donor while Au NRs were selected as the energy acceptor. The experimental results suggested that Au NRs absorbed on the surface of CDs by using cysteamine as the bridge, which turned-off the

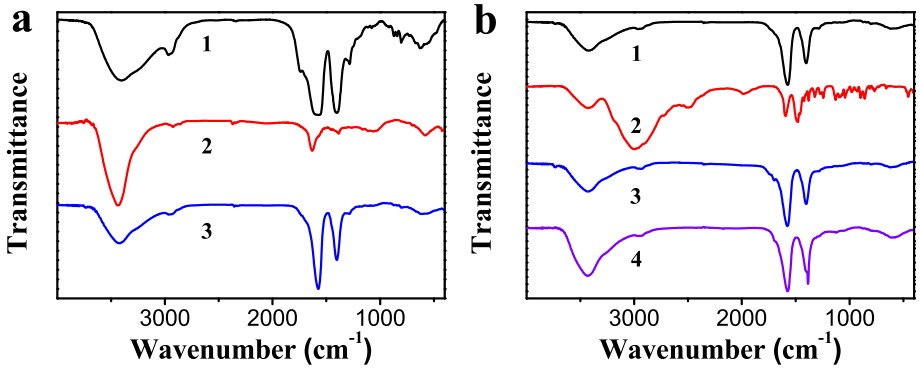

Fig. 5. (a) FT-IR spectra of synthesized CDs (curve 1), AuNRs (curve 2), and CDs/AuNRs (curve 3). (b) FT-IR spectra of synthesized CDs/AuNRs (curve 1), cysteamine (curve 2), CDs-cysteamine-AuNRs assembly (curve 3), and CDs-cysteamine-AuNRs assembly in the presence of 130 μM Pb^{2+} ions (curve 4).

Table 1
Results of the determination of Pb^{2+} ions in tap water and river water samples (n = 5)[a] by proposed CDs-cysteamine-Au NRs assembly based biosensor and traditional HPLC method (n = 5).

Sample No.	The present approach				The HPLC approach			
	Added (nM)	Measured[a] (nM)	R.S.D. (n = 5%)	Recovery (%)	Added (nM)	Measured[a] (nM)	R.S.D. (n = 5%)	Recovery (%)
Tap 1	30	29.17 ± 0.24	0.81	97.23	30	29.21 ± 0.21	0.85	97.37
Tap 2	60	62.03 ± 0.46	0.85	103.38	60	61.85 ± 0.42	0.89	103.08
Tap 3	100	103.94 ± 0.78	0.95	103.94	100	103.75 ± 0.75	0.96	103.75
River 1	40	41.11 ± 0.32	0.82	102.78	40	41.05 ± 0.31	0.87	102.63
River 2	80	83.13 ± 0.63	0.89	103.91	80	82.85 ± 0.62	0.91	103.56
River 3	120	123.75 ± 0.85	1.02	103.13	120	123.21 ± 0.83	1.00	102.68

[a] Average values are from five independent measurements ± standard deviation.

fluorescence signal due to FRET process. Interestingly, Pb^{2+} ions removed cysteamine molecules from CDs-cysteamine-Au NRs composite, which turned-on the quenched fluorescence signal of the biosensor. Based on these phenomena, the FRET-based assembly was performed as an off-on fluorescence probe for Pb^{2+} ions detection. Compared with other methods reported, our developed assay displays better performance such as label-free, simplicity, rapidity, high selectivity, and high sensitivity. Moreover, the present approach was successfully detected Pb^{2+} ions with good satisfactory results. Furthermore, this current approach provides a strategy for the design of new FRET-based fluorescent probe and possesses great potential applications in environmental monitoring fields.

Acknowledgments

We gratefully acknowledge the financial support from the National Natural Science Foundation of China (21501146), the Natural Science Foundation of Jiangsu Province (BK20150424 and BK20140464), the Opening Foundation of the Key Laboratory for Preparation and Application of Ordered Structural Materials of Guangdong Province (KLPAOSM201507), and the Opening Project of Jiangsu Key Laboratory of Biochemistry and Biotechnology of Marine Wetland (K2016-18).

Appendix. ASupplementary data

Supplementary data to this article can be found online at https://doi.org/10.1016/j.talanta.2019.03.101.

References

[1] K. Okamoto, Y. Sako, Recent advances in FRET for the study of protein interactions and dynamics, Curr. Opin. Struct. Biol. 46 (2017) 16–23.
[2] X. Zhang, C.A. Marocico, M. Lunz, V.A. Gerard, Y.K. Gun, V. Lesnyak, N. Gaponik, A.S. Susha, A.L. Rogach, A.L. Bradley, Experimental and theoretical investigation of the distance dependence of localized surface plasmon coupled Forster resonance energy transfer, ACS Nano 8 (2014) 1273–1283.
[3] K.F. Chou, A.M. Dennis, Forster resonance energy transfer between quantum dot donors and quantum dot acceptors, Sensors 15 (2015) 13288–13325.
[4] T. Ogoshi, D. Yamafuji, T. Yamagishi, A.M. Brouwer, Forster resonance energy transfer by formation of a mechanically interlocked rotaxane, Chem. Commun. 49 (2013) 5468–5470.
[5] Y.L. Chiu, S.A. Chen, J.H. Chen, K.J. Chen, H.L. Chen, H.W. Sung, A dual-emission Forster resonance energy transfer nanoprobe for sensing/imaging pH changes in the biological environment, ACS Nano 4 (2010) 7467–7474.
[6] H. Dacres, J. Wang, M.M. Dumancic, S.C. Trowell, Experimental determination of the Forster distance for two commonly used bioluminescent resonance energy transfer pairs, Anal. Chem. 82 (2010) 432–435.
[7] X. Yu, C.X. Zhang, L.N. Zhang, Y.R. Xue, H.W. Li, Y.Q. Wu, The construction of a FRET assembly by using gold nanoclusters and carbon dots and their application as a ratiometric probe for cysteine detection, Sensor. Actuator. B Chem. 263 (2018) 327–335.
[8] S.Y. Lim, W. Shen, Z.Q. Gao, Carbon quantum dots and their applications, Chem. Soc. Rev. 44 (2015) 362–381.
[9] J.J. Zhang, F.F. Cheng, J.J. Li, J.J. Zhu, Y. Lu, Fluorescent nanoprobes for sensing and imaging of metal ions: recent advances and future perspectives, Nano Today 11 (2016) 309–329.
[10] X.C. Sun, Y. Lei, Fluorescent carbon dots and their sensing applications, Trac. Trends Anal. Chem. 89 (2017) 163–180.
[11] J. Wen, Y.Q. Xu, H.J. Li, A.P. Lu, S.G. Sun, Recent applications of carbon nanomaterials in fluorescence biosensing and bioimaging, Chem. Commun. 57 (2015) 11346–11358.
[12] W.S. Zou, C.H. Ye, Y.Q. Wang, W.H. Li, X.H. Huang, A hybrid ratiometric probe for glucose detection based on synchronous responses to fluorescence quenching and resonance light scattering enhancement of boronic acid functionalized carbon dots, Sensor. Actuator. B Chem. 271 (2018) 54–63.
[13] G.L. Liu, C.L. Xuan, D.-Q. Feng, D.L. Hua, T.H. Liu, G. Qi, W. Wang, Dual-modal fluorescence and light-scattering sensor based on water-soluble carbon dots for silver ions detection, Anal. Methods 9 (2017) 5611–5617.
[14] G.L. Liu, Z. Chen, X.Y. Jiang, D.-Q. Feng, J.Y. Zhao, D.H. Fan, W. Wang, In-situ hydrothermal synthesis of molecularly imprinted polymers coated carbon dots for fluorescent detection of bisphenol A, Sensor. Actuator. B Chem. 228 (2016) 302–307.
[15] D.-Q. Feng, G.L. Liu, W. Wang, Dual-modal light scattering and fluorometric detection of lead ion by stimuli-responsive aggregation of BSA-stabilized copper nanoclusters, RSC Adv. 6 (2016) 96729–96734.
[16] M. Ganiga, J. Cyriac, FRET based ammonia sensor using carbon dots, Sensor. Actuator. B Chem. 225 (2016) 522–528.
[17] Z.J. Zhang, J. Wang, C.Y. Chen, Gold nanorods based platforms for light-mediated theranostics, Theranostics 3 (2013) 223–238.
[18] H.J. Chen, L. Shao, Q. Li, J.F. Wang, Gold nanorods and their plasmonic properties, Chem. Soc. Rev. 42 (2013) 2679–2724.
[19] L. An, Y.Y. Wang, Q.W. Tian, S.P. Yang, Small gold nanorods: recent advances in synthesis, biological imaging, and cancer therapy, Materials 10 (2017) 1372.
[20] W.H. Zhu, C.L. Xuan, G.L. Liu, Z. Chen, W. Wang, A label-free fluorescent biosensor for determination of bovine serum albumin and calf thymus DNA based on gold nanorods coated with acridine orange-loaded mesoporous silica, Sensor. Actuator. B Chem. 220 (2015) 302–308.
[21] L. Vigderman, B.P. Khanal, E.R. Zubarev, Functional gold nanorods: synthesis, self-assembly, and sensing applications, Adv. Mater. 24 (2012) 4811–4841.
[22] Y.Q. Dong, J.W. Shao, C.Q. Chen, H. Li, R.X. Wang, Y.W. Chi, X.M. Lin, Blue luminescent graphene quantum dots and graphene oxide prepared by tuning the carbonization degree of citric acid, Carbon 50 (2012) 4738–4743.
[23] X.C. Ye, Y.Z. Gao, J. Chen, D.C. Reifsnyder, C. Zheng, C.B. Murray, Seeded growth of monodisperse gold nanorods using bromide-free surfactant mixtures, Nano Lett. 13 (2013) 2163–2171.
[24] C.J. Orendorff, C.J. Murphy, Quantitation of metal content in the silver-assisted growth of gold nanorods, J. Phys. Chem. B 110 (2006) 3990–3994.
[25] X.Y. Jiang, D.-Q. Feng, G.L. Liu, D.H. Fan, W. Wang, A fluorescent switch sensor for detection of anticancer drug and ctDNA based on the glutathione stabilized gold nanoclusters, Sensor. Actuator. B Chem. 232 (2016) 276–282.
[26] X. Zhu, X.Y. Gao, Q.D. Liu, Z.Y. Lin, B. Qiu, G.N. Chen, Pb^{2+}-introduced activation of horseradish peroxidase (HRP)-mimicking DNAzyme, Chem. Commun. 47 (2011) 7437–7439.
[27] Y. Xiao, A.A. Rowe, K.W. Plaxco, Electrochemical detection of parts-per-billion lead via an electrode-bound DNAzyme assembly, J. Am. Chem. Soc. 129 (2007) 262–263.
[28] Z.Z. Lin, Y. Chen, X.H. Li, W.H. Fang, Pb^{2+} induced DNA conformational switch from hairpin to G-quadruplex: electrochemical detection of Pb^{2+}, Analyst 136 (2011) 2367–2372.
[29] T. Li, S.J. Dong, E.K. Wang, A lead(II)-driven DNA molecular device for turn-on fluorescence detection of lead(II) ion with high selectivity and sensitivity, J. Am. Chem. Soc. 132 (2010) 13156–13157.